Structural and magnetic resonance investigations of $CuCr_2S_4$ nanoclusters and nanocrystals

Cite as: J. Appl. Phys. **116**, 054302 (2014); https://doi.org/10.1063/1.4891993
Submitted: 25 June 2014 . Accepted: 22 July 2014 . Published Online: 04 August 2014

A. I. Pankrats, A. M. Vorotynov, V. I. Tugarinov, S. M. Zharkov, D. A. Velikanov, G. M. Abramova, G. M. Zeer, K. Ramasamy, and A. Gupta

Structural and magnetic resonance investigations of $CuCr_2S_4$ nanoclusters and nanocrystals

A. I. Pankrats,[1,2,a)] A. M. Vorotynov,[1] V. I. Tugarinov,[1] S. M. Zharkov,[1,2] D. A. Velikanov,[1,2] G. M. Abramova,[1] G. M. Zeer,[2] K. Ramasamy,[3] and A. Gupta[3]
[1]*Kirensky Institute of Physics, SB RAS, Akademgorodok, Krasnoyarsk 660036, Russia*
[2]*Siberian Federal University, 79 Svobodny prosp., Krasnoyarsk 660041, Russia*
[3]*MINT Center, The University of Alabama, Tuscaloosa, Alabama 35487, USA*

(Received 25 June 2014; accepted 22 July 2014; published online 4 August 2014)

Nanoclusters and nanocrystals of the room temperature magnetic spinel $CuCr_2S_4$ synthesized using a facile solution-based method have been examined by transmission electron microscopy, magnetic measurements, and magnetic resonance over a wide frequency range 9.6–80 GHz and at temperatures down to 4.2 K. Decreasing of the resonance field and broadening of the resonance lines below 50 K for both samples are due to the freezing of magnetic moments of nanocubes and nanocrystalline particles constituting nanoclusters. The effective fields of averaged magnetic anisotropy $\langle H_A \rangle \cong 2.4$ kOe are similar for both nanopowder samples as estimated from resonance measurements at T = 4.2 K. An additional blocking temperature $T_b \cong 300$ K appears in nanoclusters due to freezing of the magnetic moment of the entire cluster as a whole. Below this blocking temperature, the magnetic dipolar field acting in boundary areas of interacting constituent nanocrystals is responsible for the additional low-field resonance line observed in the resonance spectra of nanoclusters at X-band. © *2014 AIP Publishing LLC*. [http://dx.doi.org/10.1063/1.4891993]

I. INTRODUCTION

The physics of nanoscale magnetic materials has been an active research subject in the last few decades not only for technological reasons but also from fundamental research point of view. In the last decade, detailed investigations have been carried out in the field of nano-sized magnetic particles, because of their various promising applications in ferrofluids, high-frequency electronics, high performance permanent magnets, and magnetic storage devices.[1–3] Magnetic particles are also attractive for use in biology and medical applications such as drug-targeting, cancer therapy, lymph node imaging, and hyperthermia.[1,4]

The study of an ensemble of single-domain magnetic nanoparticles is of particular interest.[5] Such nanoparticle behaves like a small permanent magnet whose magnetic moment can be up to 10^5 Bohr magneton (μ_B). A system consisting of non-interacting single-domain particles is characterized by superparamagnetic behavior with instability of the magnetization due to thermal agitation.[6,7] At temperatures below a certain blocking temperature, the directions of the individual magnetic moments of the particles are frozen and, in general, are distributed randomly due to the distribution of the easy axis of magnetic anisotropy for individual particles.

If the interaction between the particles cannot be neglected, their magnetic properties can be determined by the dipole field energy along with the thermal and magnetic anisotropy energies. At sufficiently high packing densities, the inter-particle interactions have profound effects on the spin dynamical properties of the particle assembly. In this case, the inter-particle interactions not only modify the energy barrier arising from the anisotropy contributions of each particle but may produce a low temperature collective state that is completely different from the individual blocked one.[7–9]

The magnetic resonance properties of non-interacting or weakly interacting magnetic nanoparticles are currently the subject of intense experimental and theoretical studies (see, e.g., Refs. 10–12).

In this paper, we present results of the investigation of the magnetic resonance and structural properties of $CuCr_2S_4$ nanopowder. Among the chalcospinels, Cu- and Cr-based systems are unique in that they are ferromagnetic metals at room temperature with Curie temperatures (T_C) of 377, 430, and 360 K for $CuCr_2S_4$, $CuCr_2Se_4$, and $CuCr_2Te_4$, respectively. As for Cu-Cr-S system, depending on the synthesis conditions, pure disulphide $CuCrS_2$ or spinel $CuCr_2S_4$ compounds can be obtained separately, but a mixture of the two phases is also possible. In the case of the latter, the nature of formation of the $CuCr_2S_4$ phase in the bulk $CuCrS_2$ matrix depends also on the synthesis conditions. It may form large volume areas, thin layers, or islands, which are uniformly or randomly distributed in the $CuCrS_2$ matrix.[13,14] It was shown recently[15] that pure-phase $CuCr_2S_4$ spinel in the form of nanocubes or nanoclusters can be obtained by solution chemistry with choice of specific synthesis solvents.

Our resonance and structural studies show that below 50 K, magnetic freezing occurs in both the nanocubes and smaller particles constituting nanocluster samples. The freezing of the magnetic moments causes a low temperature shift of the resonance fields and broadening of resonance lines. An additional blocking behavior around 300 K appears in

a)E-mail: pank@iph.krasn.ru

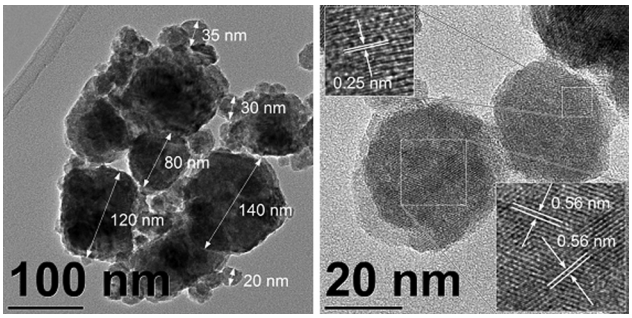

FIG. 1. TEM (a) and HRTEM (b) images of $CuCr_2S_4$ OLA nanopowders.

nanoclusters due to freezing of the magnetic moment of the whole nanocluster, whose averaged anisotropy determines the energy barrier between the states. Below this blocking temperature, an additional low-field resonance line is observed in the resonance spectra of nanoclusters at X-band due to the additional dipolar field acting in the boundary areas of the interacting constituent nanocrystals.

II. SYNTHESIS OF $CuCr_2S_4$ NANOCLUSTERS AND NANOCRYSTALS

The synthesis of nanopowdered $CuCr_2S_4$ is described in detail in Ref. 15, where using oleylamine (OLA) as a solvent yielded nanoclusters with an average size of 31 ± 2.5 nm, while with octadecylamine (ODA), cube-shaped nanocrystals with an average size of 20 ± 2 nm were obtained.

The phase purity of the synthesized nanocubes and nanoclusters was confirmed by powder X-ray diffraction,[15] which indicated the expected spinel structure (fcc, space group $Fd3m$) with lattice parameters 9.922Å and 9.916 Å for ODA- and OLA-capped particles, respectively.

The morphology and structure of the nanoclusters and nanocrystals were investigated by high resolution transmission electron microscopy (HRTEM). The cube-shaped nanocrystals prepared using ODA as a solvent are defined as nearly perfect cubic-shaped particles with size of 20 ± 2 nm (edge-to-edge). The TEM images of the cube-shaped nanocrystals and their detailed description can be found in Ref. 15.

The morphology of nanopowder prepared using OLA and used in this study differs from that mentioned in Ref. 15, where only nanoclusters with the average size of 31 ± 2.5 nm composed of oblate shaped smaller particles were found. We found the nanoclusters with sizes from 80 to 140 nm composed of smaller particles (Fig. 1(a)), which are on the average larger than those in Ref. 15. In addition, some nanocrystals with sizes approximately varying from 15 to 40 nm that appear like single crystals are observed in Figs. 1(a) and 1(b). The measured distance between the lattice fringes from the HRTEM image in Fig. 1(b) is 0.56 nm corresponding to the (111) planes of cubic $CuCr_2S_4$. Moreover, lattice fringes with distance of 0.25 nm between them, corresponding to the (400) planes, are clearly visible in the neighbor particle in Fig. 1(b). From energy-dispersive spectroscopy (EDS) analysis, all particles correspond to the chemical compound $CuCr_2S_4$.

III. EXPERIMENTAL RESULTS

In the temperature range 77–370 K, the resonance spectra were collected with a Bruker spectrometer (Elexsys E580) operating at X- and Q-band ($\nu = 9.7$ and 36 GHz, respectively) using 100 kHz modulation frequency. The temperature evolutions of the X-band spectra of the $CuCr_2S_4$ nanoclusters and nanocubes are shown in Fig. 2.

Fig. 2 shows the appearance of resonance lines at 350 K and 360 K for the nanoclusters and nanocrystals, respectively, which can be ascribed to the T_C. These values are in agreement with the T_C's reported in Ref. 15 and somewhat lower than the bulk value of 377 K.[16,17] Lowering of the Curie temperature in comparison with the bulk substance can be attributed to the nanometer scale size of the particles that leads to the strong influence of the demagnetizing factors and surface effects. With lowering the temperature, a single line with an almost Lorentz shape is observed for the nanocubes at all temperatures, while two resonance peaks can be seen at temperatures below 300 K for the nanoclusters spectra. Fig. 3 shows the temperature dependence of the resonance fields for two clearly visible resonance peaks of the nanocluster sample. In contrast, the resonance spectrum for the nanoclusters measured at temperatures $120 < T < 300$ K in Q-band is a single line.

The resonance linewidth of the nanocube sample measured at X-band increases monotonously with decreasing

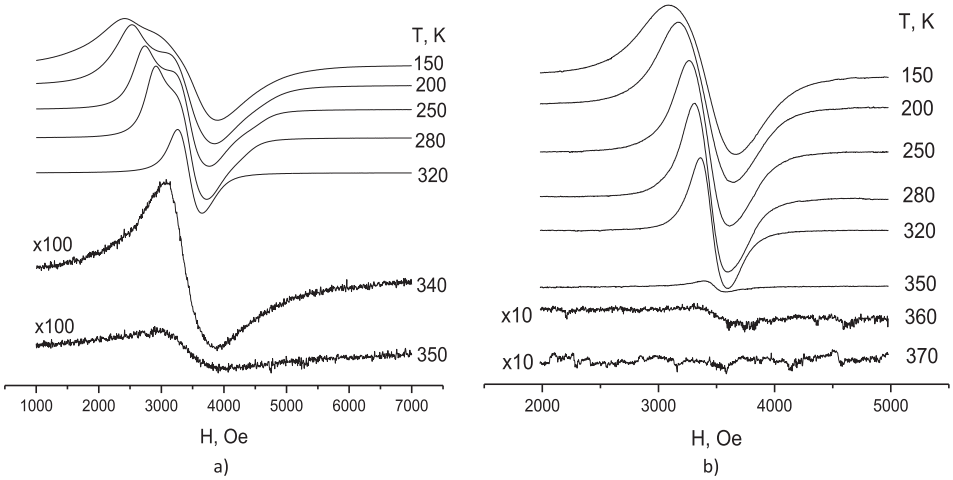

FIG. 2. Temperature evolutions of the X-band spectra: (a) nanoclusters, (b) nanocubes.

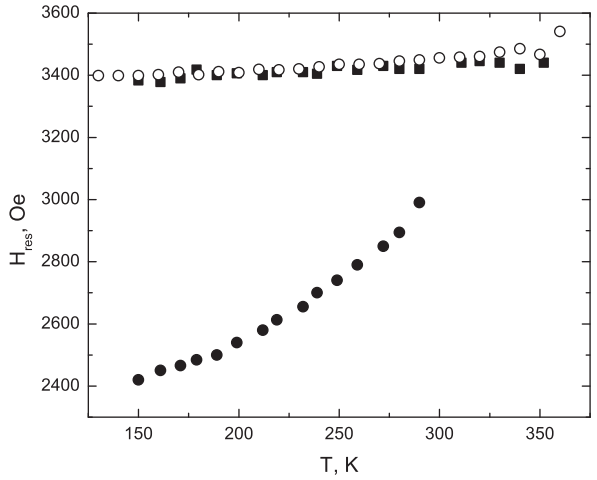

FIG. 3. Temperature dependencies of the resonance fields measured at X-band for the two resonance peaks for nanoclusters (closed circles and squares). Open circles present the resonance fields for the nanocubes.

temperature (see Fig. 4). It is seen qualitatively from Fig. 2 that the widths of the individual lines in the resonance spectrum for nanoclusters also increase with decreasing temperature. However, the resonance spectrum at temperatures below 300 K is poorly described by the sum of two Lorentzian or Gaussian shaped lines. Therefore, the temperature dependence of the linewidth for the nanocluster sample is given only for the more pronounced high-field resonance line.

At low temperatures, the resonant properties of the nanocluster and nanocubes were studied over a wide frequency range using a magnetic spectrometer with pulsed magnetic field.[18] The frequency-field and temperature dependencies of the magnetic resonance were investigated.

The frequency-field dependencies measured for the nanoclusters and nanocubes at T = 4.2 and 80 K are shown in Fig. 5. The inset shows the dependencies for the nanoclusters over an extended frequency range. For both the nanocluster and nanocube samples, the dependencies are linear at both temperatures and gapless at T = 80 K. At T = 4.2 K, the

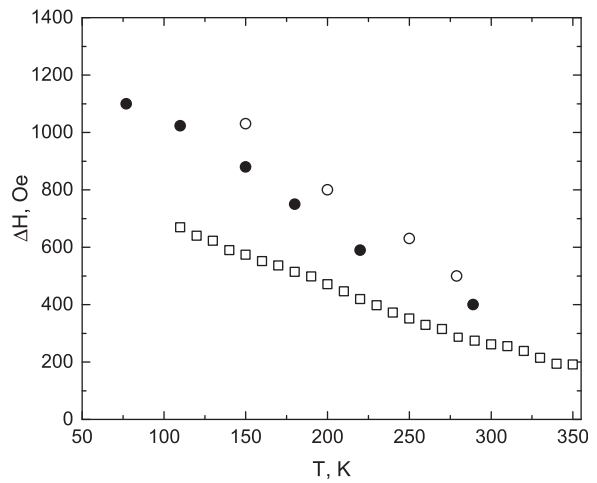

FIG. 4. Temperature dependences of the resonance linewidths measured at X-band: open squares—nanocubes, closed circles—nanoclusters + mMgCO3·Mg(OH)2·nH2O (X-band), open circles—nanoclusters, high-field resonance line.

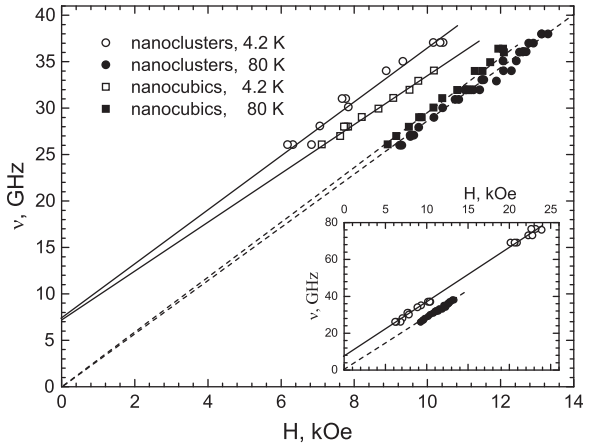

FIG. 5. Frequency-field dependencies measured for the nanocluster and nanocubes at T = 4.2 and 80 K.

energy gap of the resonance spectra is $\nu_c \approx 7$ GHz for both samples.

The temperature dependencies of the resonance fields have been measured for the nanocluster and nanocube samples at various frequencies. To compare them, we represent the data normalized to the value at T = 80 K as shown in Fig. 6. The resonance field values decrease below ~50 K for both the nanocube and nanocluster samples. The temperature shift of the resonance field is weaker for the nanocubes than in the nanoclusters, which is in accordance with the respective frequency-field dependencies (see Fig. 5).

The typical temperature dependencies of the linewidths for the nanocluster and nanocube samples are depicted in Fig. 7. It can be seen that the linewidths for both samples increase monotonically with decreasing temperature below approximately 80 K, and the resonance line width is greater for the nanoclusters.

For all the resonance measurements, no dependence of the resonance parameters on cooling condition (ZFC or FC) was observed in contrast with the magnetization data.[15] This suggests that the energy barriers between ZFC and FC states are much smaller than the energy of the field values used for the resonance experiments.

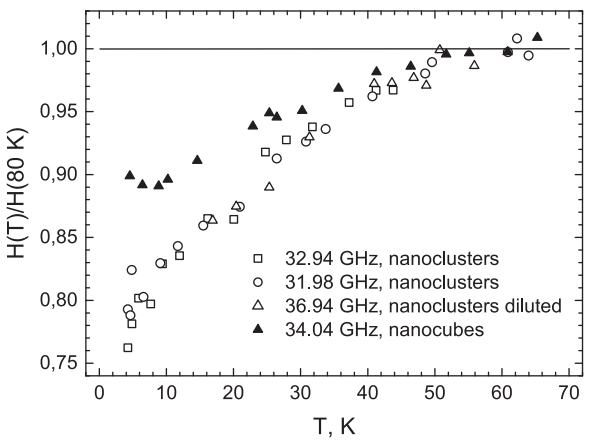

FIG. 6. Temperature dependencies of the resonance fields for the nanocluster and nanocube crystals normalized to T = 80 K.

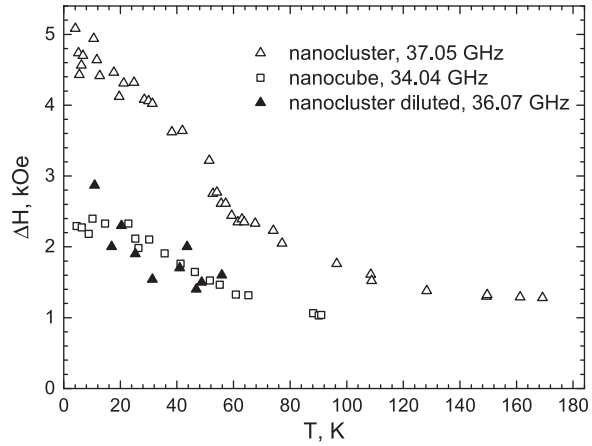

FIG. 7. Temperature dependencies of the linewidths for the nanocluster and nanocube samples.

IV. DISCUSSION

Our experimental data show that at low temperatures (below ~50 K), the resonance properties of the nanoclusters and nanocubes have the same features: the formation of gap character in the resonance spectrum and significant broadening of the resonance lines with decreasing temperature. On the other hand, at high temperatures (above 50 K), a splitting of the resonance spectrum into two lines is observed at X-band for the nanocluster sample only, along with a strong decrease of the resonance field for the low-field line with decreasing temperature. In contrast, the single resonance line for the nanocubes exhibits almost temperature-independent resonance field at $T > 50$ K.

The appearance of two resonance lines in the nanoclusters below ~300 K cannot be attributed to the anisotropic g-value (for example $g_{||}$ and $g_{\perp}$). In the case of the anisotropic g-value, the splitting of the resonance spectra should increase with increasing resonance frequency. However, a single resonance line is obtained when measured in Q-band at temperatures of $120\,\text{K} < T < 300\,\text{K}$. Notice, however, that the linewidth in Q-band is more than approximately twice larger in comparison with the X-band.

The interpretation of the results can be made based on comparison of the magnetic properties of the nanocluster and nanocube samples. The temperature dependences of ZFC and FC magnetizations were measured with a SQUID magnetometer in fields of 50–500 Oe for the nanoclusters (Fig. 8(a)) and nanocubes (Fig. 8(b)): A comparison of the samples. These peaks define the values of the blocking temperature Tb, which is close for both samples (approximately 30–50 K). However, the magnetizations of the nanocluster and nanocube samples differ substantially in the temperature range 60–300 K. There is an additional distinct high-temperature peak in the ZFC magnetization for the nanocluster sample at a temperature of approximately 290 K, which is absent in the nanocube sample. The temperature dependencies of the ZFC and FC magnetization of the nanocubes are typical for the superparamagnetic state at temperatures above 60 K. Most likely, the slight difference between the ZFC and FC magnetizations that appears below 200 K can be explained by the dispersion of the particle sizes.

The appearance of the blocking temperature is typical for superparamagnetic particles.[5,6] They will manifest in the properties of superparamagnetism if the time τ for change of the direction of the magnetization of the particle due to thermal fluctuations is comparable to or less than the characteristic measurement time τ_m. The characteristic time of the inversion of the magnetization of a single domain particle of volume V and anisotropy constant K_{eff} can be estimated from the Néel–Brown relation,[19] which is valid for non-interacting particles:

$$\tau = \tau_0 \exp\left(\frac{K_{eff}V}{k_B T}\right), \tag{1}$$

where k_B is Boltzmann's constant and the typical values of the characteristic flip time τ_0 depend on parameters such as the temperature, magnetization, gyromagnetic ratio, anisotropy constant, etc., and are in the interval 10^{-13}–10^{-10} s.[5,6] From this expression, the volume of the particle can be estimated as

$$V = \ln\left(\frac{\tau_m}{\tau_0}\right)\frac{k_B T}{K_{eff}}. \tag{2}$$

Thus, it follows that the blocking temperature is determined by the size of the particle with other parameters being equal. Consequently, there are two characteristic dimensions in the nanocluster samples that define two different blocking temperatures.

We assume that the low blocking temperature is determined by the freezing of the magnetization directions in the

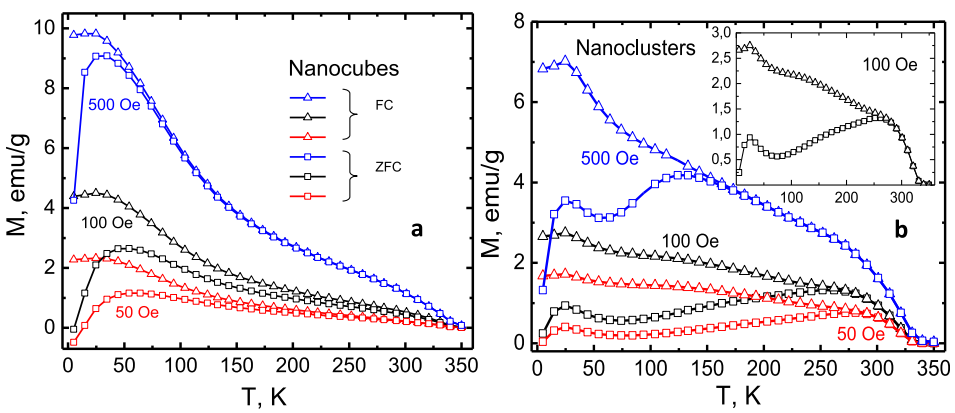

FIG. 8. Temperature dependences of FC and ZFC magnetizations in the nanocubes (a) and nanoclusters (b).

nanocubes or the smaller particles constituting the nanoclusters. Thus, the gapped character of the magnetic resonance found for both the nanocluster and nanocube samples below 50 K is related to the blocked state, and the gap is defined by the mean value of the anisotropy field:[20]

$$\omega/\gamma = H + \langle H_A \rangle. \quad (3)$$

A similar behavior of the resonance spectra was previously observed for many ensembles of nanoparticles.[10,11,21,22] The similar values of $\langle H_A \rangle \cong 2.4$ kOe for both samples can be estimated from the resonance data of Fig. 5 at T = 4.2 K. This value is close to that found in bulk chalcogenide spinel.[23] Using the value of the saturation magnetization of a nanocube of $M_S \cong 30$ emu/g[15] results in $|K_{eff}| \cong 1 \times 10^5$ erg/cm^3. Additionally, with the conventional value of $\tau_m = 10$ s for dc magnetization measurements in Ref. 15 and $T_b = 50$ K, we can estimate the particle size of the nanocubes from the Eq. (2) to be $D_{ncube} \cong 12$ nm. This value is appreciably lower than $D_{ncube} \cong 20 \pm 2$ nm found in Ref. 15 by TEM. Note that the similar low-temperature blocking with $T_b \cong 30$ K was observed in $CuCr_2S_4$ powder consisting of crystallites with size of about 8 nm prepared by mechanical alloying.[24] For a more accurate estimation of the particle sizes from the Néel–Brown Eq. (1) or Vogel-Fulcher equations,[25] the ac-magnetization measurements over a wide frequency range should be used (see, for example, Ref. 26).

Note also that the frequency-field dependences of the resonance for both nanoclusters and nanocubes at T = 4.2 K show comparable values of the energy gap, which are determined by similar values of the averaged anisotropy field (3). Thus, the similar sizes of the nanocubes and nanocrystalline particles constituting the nanocluster determine the close values of the blocking temperature (about 50 K) and the similar low-temperature resonance properties of these two materials.

Most likely, another characteristic size which can result in the high blocking temperature near 300 K in nanoclusters is the size of a cluster. Due to the compact arrangement of the constituent particles in the cluster, the interaction between them becomes significant. The primary type of interaction is dipole-dipole type, but the exchange interaction contribution between the particles can also be noticeable for a high degree of compactness.[5] As a result, ferromagnetic ordering of the cluster can occur, and the cluster can be considered as a superferromagnetic particle.[5] Estimates show that the magnetic moment of a cluster with an average size of 100 nm could reach $\sim 10^7 \mu_B$.

Based on the average cluster size of 100 nm and a blocking temperature of 300 K, we can estimate the value of the anisotropy constant for the cluster that determines the energy barrier between the two easy-axis states. The obtained value of $K_{eff} = 1 \times 10^3$ erg/cm^3 is two orders of magnitude less than the anisotropy constant for the individual particle of a cluster estimated at T = 4.2 K. The magnetic anisotropy of a cluster as a whole can have two main contributions: (i) the shape anisotropy of the cluster and (ii) the anisotropy averaged over the entire ensemble of particles constituting the cluster. The shape anisotropy of the cluster is negligible due to its nearly spherical shape. The magnetic anisotropy of the individual particles at 300 K is small due to the proximity of the Curie temperature (see, for example, Ref. 23). Moreover, the averaging of the anisotropy over the cluster results in an additional decrease of the anisotropy because of the random orientations of the easy axes of individual particles.

Due to the compact arrangement of constituent nanocrystals in a cluster, the interaction between the nanocrystals is significant. We assume that the boundary areas of the constituent nanocrystals are in the effective field determined by the sum of the external magnetic field H_{ext} and the additional effective field due to the interactions between particles $H_{int}(T)$.

$$H_{eff} = H_{ext} + H_{int}(T). \quad (4)$$

The energy of the dipole-dipole interaction, which provides the main contribution to the interaction between the particles, is proportional to r^{-3}, where r is the distance between the centers of the particles. Hence, it is clear that the strongest effective field of the dipole-dipole interaction acts in the border areas of neighboring particles and decreases down rapidly inside them. In the closely packed cluster, every particle is surrounded by up to 12 neighboring ones. This means that the boundary areas of the constituting particles are situated in an effective field H_{eff} (4).

We believe that the resonance absorption in these areas is the reason for appearance of the low-field resonance peak of the resonance spectra in the nanoclusters. The low intensity of this resonance line reflects the fact that only boundary areas of nanocrystals are under the effect of dipolar interaction. The dipolar field $H_{d\text{-}d}(T)$ depends on the temperature as $H_{d\text{-}d}(T) \sim M_S(T)$, where M_S is the saturation magnetization, and its increase with decreasing temperature defines the temperature dependence of the resonance field for the low-field resonance line (see Fig. 3). The effective field resulting from interactions between the smaller particles of nanoclusters is estimated from the temperature dependence of the resonance field in Fig. 3 using Eq. (4): $H_{int} \cong 1000$ Oe at T = 150 K. As it follows from formula (4), the same shift of the low-field resonance peak should be observed with decreasing temperature in the Q-band.

However, the additional line is not resolved because of the large linewidths at these frequencies.

Strictly speaking, the interaction between the particles can exist not only inside the cluster but also between the neighboring clusters in which the magnetic moments are also frozen. However, such interaction will be weaker due to the fact that the distances between the clusters are significantly greater than those between the particles in a compact cluster. The visible second resonance peak in the resonance spectra of the cube-shaped nanocrystals is absent at temperatures 150–300 K, where they are superparamagnetic, as it readily follows from Fig. 8(a).

The field dependences of magnetization measured at various temperatures (Fig. 9) confirm the proposed scenario of the behavior of nanocluster and nanocube ensembles. Non-hysteretic magnetization curves are observed for both samples at T = 318 K (Fig. 9(b) and 9(d)) confirming the superparamagnetic behavior of both nanocube and

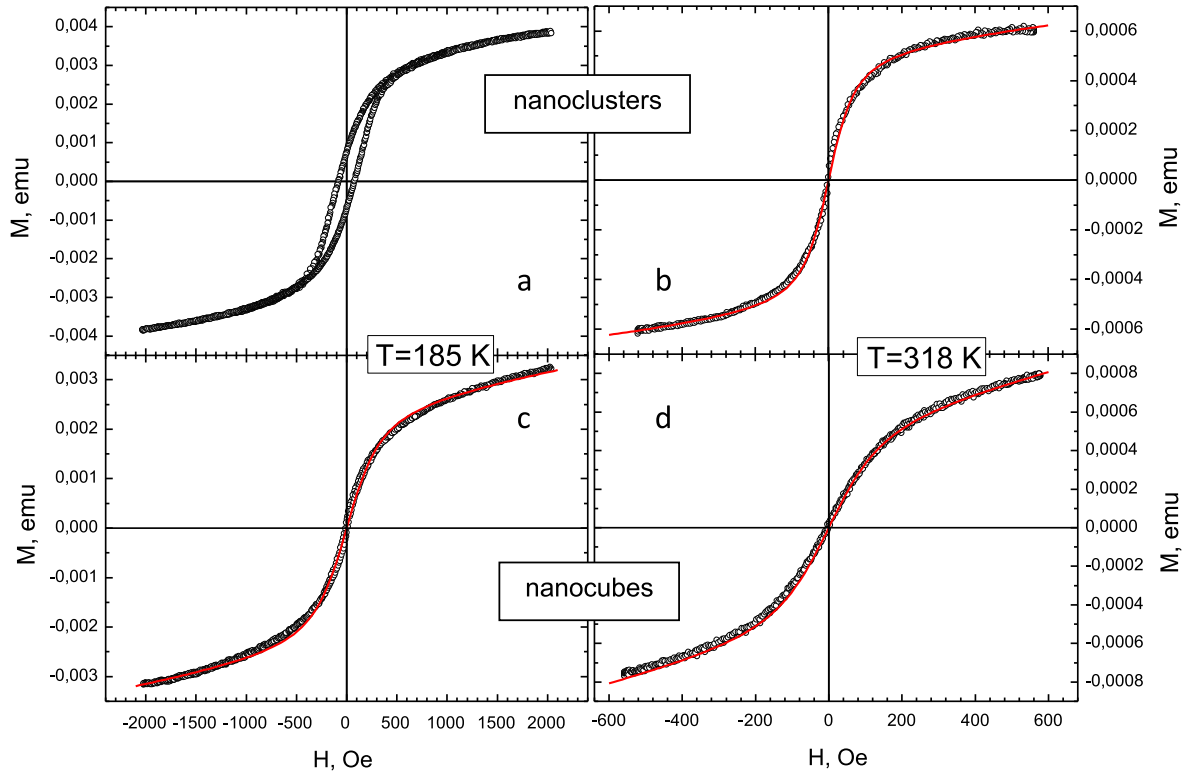

FIG. 9. Field dependencies of magnetizations of the nanoclusters and nanocubes at 185 and 318 K. The red lines correspond to the Langevin fits.

nanocluster ensembles. At T = 185 K, i.e., below the high blocking temperature near 300 K, a distinct ferromagnetic hysteresis loop with coercivity value of ~80 Oe is obtained for the nanoclusters (Fig. 9(a)). However, the field dependence for the nanocubes remains non-hysteretic at the same temperature (Fig. 9(c)).The red lines in Figs. 9(b)–9(d) correspond to the Langevin fits. At T = 5 K, the magnetization of both ensembles of nanoparticles are frozen and the corresponding field dependences as they are presented in Ref. 15 possess a typical hysteretic behavior. Interestingly, the average size of the nanocubes estimated from the Langevin fit at T = 185 K is equal to 16.5 nm that is rather close to our estimation from the blocking temperature. There is little sense in a similar estimation for the nanoclusters since they are unlikely to remain single-domain.

To decrease the influence of interparticle magnetic interactions between the constituent nanocrystals in a cluster, the$CuCr_2S_4$nanocluster sample was diluted by nonmagnetic fine powdered magnesium carbonate $mMgCO_3{\cdot}Mg(OH)_2{\cdot}nH_2O$ in ratio ($CuCr_2S_4$): ($mMgCO_3{\cdot}Mg(OH)_2{\cdot}nH_2O$) ≅ 1:20. Thereafter, the obtained mixture was thoroughly ground in the agathic mortar. Figs. 10(a) and 10(b) show TEM images with different magnification of $CuCr_2S_4$ nanoclusters after such treatment. It is seen that the majority of the clusters are destroyed and mainly well separated nanocrystals, with dimensions of 20–40 nm (see Fig. 10(b)), are observed in the background of the magnesium carbonate plates.

The resonance measurements of the diluted sample carried out at X-band under the same conditions as for the original nanoclusters sample confirm such transformation (see Fig. 11). In contrast with the original nanoclusters sample spectra (see Fig. 2(a)), a single line is observed at all temperatures down to 77 K. The temperature dependence of the

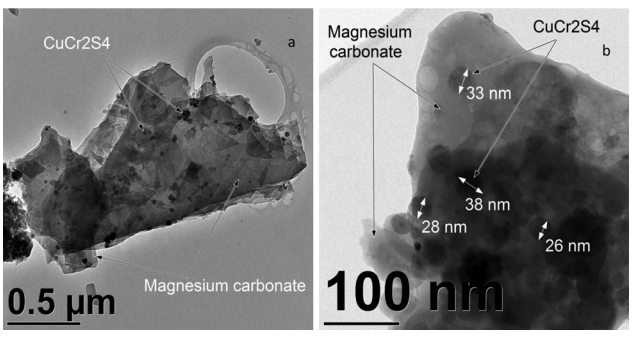

FIG. 10. TEM images ((a) and (b)) of $CuCr_2S_4$ nanoclusters after diluting with magnesium carbonate and grinding.

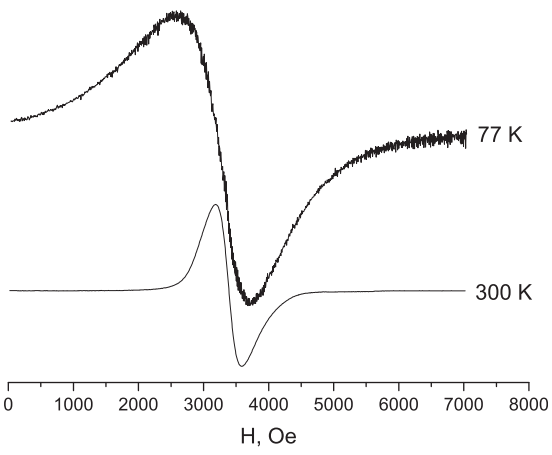

FIG. 11. Resonance spectra of the diluted sample at two different temperatures.

linewidth of the diluted sample measured at X-band is depicted by closed circles in Fig. 4. However, it appears that some amount of the nanoclusters remains unaltered. Therefore, at T = 77 K, the resonance line is slightly asymmetrical, the low-field part of the line is more expanded due to the contribution of the dipolar interaction in the residual clusters in contrast with the room temperature resonance line, which is of the Lorentz type and symmetrical.

The temperature dependencies of the resonance linewidths at X-band (see Fig. 4) also reflect the influence of the local magnetic fields (Eq. (4)). For all the investigated samples (cube-shaped nanocrystals, nanoclusters, and diluted nanoclusters), the linewidth increases monotonously with decreasing temperature. Over the entire temperature range (Fig. 4), the nanocluster samples have the highest values of the linewidth, the cube-shaped nanoparticles—the smallest ones, and the linewidth of the diluted nanocluster samples have intermediate values. The same ratio of the linewidths is maintained at temperatures below 60 K. As follows from Fig. 7, the resonance linewidths of the nanocubes and diluted nanoclusters at T = 4.2 K amount to approximately 2.5 kOe, which is close to the average value of the anisotropy field found from the resonance measurements. At the same time, the linewidth for the nanoclusters is approximately twice as high due to the dipole interaction contribution between the constituent nanoparticles. However, as is seen from Fig. 4, extrapolation to the Curie temperature where the contribution of the dipolar interaction becomes negligible gives the linewidths at X-band equal for all samples, $\Delta H \cong 180$ Oe.

At the same time below 60 K, the frequency-field and temperature dependencies of the resonance properties for the diluted nanocluster sample coincide with that of the original nanocluster sample. For example, the temperature dependence of the resonance field measured for the diluted nanocluster sample is shown in Fig. 6 by open triangles.

The interpretation given above explains the appearance of a high blocking temperature by the freezing of magnetic moment of the whole nanocluster whose averaged anisotropy determines the energy barrier between the states. Note that below the freezing temperature of the magnetic moment of the whole cluster, the principal line of the magnetic resonance spectrum should be also shifted to smaller magnetic fields according to Eq. (3), as it occurs at lower temperatures. However, unlike the low temperature range, this shift is negligible due to the small estimated value of the magnetic anisotropy of the cluster.

It is known that a sharp increase in the anisotropy constant occurs in bulk copper-chromium spinel with decreasing temperature.[23] This leads to the fact that at low temperatures the anisotropy of the constituent nanocrystal particles of the clusters becomes substantial, and at $T < \sim 50$ K, the freezing of the magnetic moments occurs in the particles constituting the clusters and in the individual single-crystal nanoparticles existing in the OLA-sample.

V. CONCLUSIONS

Nanoclusters and nanocrystals of the room temperature magnetic spinel $CuCr_2S_4$ synthesized using a facile solution-based method were examined by transmission electron microscopy and by magnetic resonance in a wide frequency range 9.6–80 GHz and at temperatures down to 4.2 K. The lowering of the magnetic phase transition temperature T_C down to 350 K and 360 K (for nanoclusters and nanocrystals, respectively) in comparison with the bulk substance was confirmed.

Decreasing of the resonance field and broadening of the resonance lines are found below ~50 K for both the nanocluster and nanocube samples. These phenomena are typical for superparamagnetic particles and are explained by the freezing of magnetic moments of the particles (nanocubes and nanocrystalline particles constituting the nanoclusters) due to the magnetic anisotropy. Similar values were estimated for both nanopowder samples effective field of the averaged magnetic anisotropy $\langle H_A \rangle \cong 2.4$ kOe from the resonance measurements at T = 4.2 K.

It was shown that an additional blocking temperature $T_b \cong 300$ K appears in the nanoclusters, likely due to the freezing of the magnetic moment of the whole nanocluster whose averaged anisotropy determines the energy barrier between the states. Below this blocking temperature, an additional low-field resonance line was found in the resonance spectra of the nanoclusters at X-band. The additional line is related to the effective field acting in the boundary areas of the constituent particles due to their mutual interaction. The effective field originates mainly from the dipolar interaction and amounts to $H_{int} \cong 1000$ Oe at T = 150 K. The additional resonance line is absent in the nanocubes and disappears in the nanoclusters after dilution with magnesium carbonate and grinding.

ACKNOWLEDGMENTS

The work was supported by a Grant CRDF–SB RAS «New Nano-size and Layered Cu-containing Sulphides for Electronics» RUP1-7054-KR-11, N 16854. S.M.Z. acknowledges support from the Ministry of education and science of the Russian Federation (in the framework of the state assignment for SFU for 2014).

[1]C. C. Berry and A. S. G. Curtis, J. Phys. D: Appl. Phys. **36**, R198 (2003).
[2]A. J. Zarur and J. Y. Ying, Nature. **403**, 65 (2000).
[3]A. Moser, K. Takano, D. T. Margulies, M. Albrecht, Y. Sonobe, Y. Ikeda, S. Sun, and E. E. Fullerton, J. Phys. D: Appl. Phys. **35**, R157 (2002).
[4]P. Tartaj, M. del, P. Morales, S. Veintemillas-Verdaguer, T. Gonzalez-Carreno, and C. J. Serna, J. Phys. D: Appl. Phys. **36**, R182 (2003).
[5]S. Bedanta and W. Kleemann, J. Phys. D: Appl. Phys. **42**, 013001 (2009).
[6]P. E. Jönsson, Adv. Chem. Phys. **128**, 191 (2004).
[7]J. L. Dormann, R. Cherkaoui, L. Spinu, M. Nogues, F. Lucari, F. D'Orazio, D. Fiorani, A. Garcia, E. Tronc, and J. P. Jolivet, J. Magn. Magn. Mater. **187**, L139 (1998).
[8]W. Kleemann, O. Petracic, C. Binek, G. N. Kakazei, Y. G. Pogorelov, J. B. Sousa, S. Cardoso, and P. P. Freitas, Phys. Rev. B **63**, 134423 (2001).
[9]O. Petracic, X. Chen, S. Bedanta, W. Kleemann, S. Sahoo, S. Cardoso, and P. P. Freitas, J. Magn. Magn. Mater. **300**, 192 (2006).
[10]R. Berger, J. Kliava, and J.-C. Bissey, J. Appl. Phys. **87**, 7389 (2000).
[11]R. Berger, J.-C. Bissey, J. Kliava, H. Daubric, and C. Estournes, J. Magn. Magn. Mater. **234**, 535 (2001).
[12]V. N. Krivoruchko, A. I. Marchenko, and A. A. Prokhorov. Low Temp. Phys. **33**, 433 (2007).
[13]G. Abramova, A. Pankrats, G. Petrakovskii, J. C. E. Rasch, M. Boehm, A. Vorotynov, V. Tugarinov, R. Szumszak, A. Bovina, and V. Vasil'ev, J. Appl. Phys. **107**, 093914 (2010).

[14]A. M. Vorotynov, G. M. Abramova, A. I. Panktats, G. A. Petrakovskii, S. M. Zharkov, G. M. Zeer, V. I. Tugarinov, M. V. Rautskii, and V. V. Sokolov, J. Exp. Theor. Phys. **117**, 879 (2013).
[15]K. Ramasamy, D. Mazumdar, Z. Zhou, Y.-H. A. Wang, and A. Gupta, J. Am. Chem. Soc. **133**, 20716 (2011).
[16]J. B. Goodenough, Solid State Commun. **5**, 577 (1967).
[17]P. K. Baltzer, H. W. Lehmann, and M. Robbins, Phys. Rev. Lett. **15**, 493 (1965).
[18]V. I. Tugarinov, I. Ya. Makievskii, and A. I. Pankrats, Instrum. Exp. Techniq. **47**, 472 (2004).
[19]W. F. Brown, Phys. Rev. **130**, 1677 (1963).
[20]G. Petrakovskii, V. Piskorskii, V. Sosnin, and I. Kosobudskii, Fizika Tverdogo Tela, Russia **25**, 3256 (1983).
[21]Y. Raikher and V. Stepanov, Phys. Rev. B **50**, 6250 (1994).
[22]F. Gazeau, J. C. Bacri, F. Gendron, R. Perzynski, Yu. L. Raikher, V. I. Stepanov, and E. Dubois, J. Magn. Magn. Mater. **186**, 175 (1998).
[23]I. Nakatani, H. Hose, and M. Masumoto, J. Phys. Chem. Solids. **39**, 743 (1978).
[24]M. Muroi, R. Street, and P. G. McCormick, Phys. Rev. B **63**, 052412 (2001).
[25]S. Shtrikman and E. P. Wolfarth, Phys. Lett. A **85**, 467 (1981).
[26]K. Nadeem, H. Krenn, T. Traussnig, R. Wurschum, D. V. Szabo, and I. Letofsky-Papst, J. Magn. Magn. Mater. **323**, 1998 (2011).